A novel mode of nuclease action is revealed by the bacterial Mre11/Rad50 complex

9804–9816 *Nucleic Acids Research, 2015, Vol. 43, No. 20* *Published online 28 August 2015*
doi: 10.1093/nar/gkv855

A novel mode of nuclease action is revealed by the bacterial Mre11/Rad50 complex

Chew Theng Lim[1], Pey Jiun Lai[1], David R. F. Leach[2], Hisaji Maki[1] and Asako Furukohri[1,*]

[1]Division of Systems Biology, Graduate School of Biological Sciences, Nara Institute of Science and Technology, Ikoma, Nara, 630-0192, Japan and [2]Institute of Cell Biology, School of Biological Sciences, University of Edinburgh, Kings Buildings, Edinburgh EH9 3JR, UK

Received April 4, 2015; Revised July 13, 2015; Accepted August 12, 2015

ABSTRACT

The Mre11/Rad50 complex is a central player in various genome maintenance pathways. Here, we report a novel mode of nuclease action found for the *Escherichia coli* Mre11/Rad50 complex, $SbcC_2/D_2$ complex (SbcCD). SbcCD cuts off the top of a cruciform DNA by making incisions on both strands and continues cleaving the dsDNA stem at ∼10-bp intervals. Using linear-shaped DNA substrates, we observed that SbcCD cleaved dsDNA using this activity when the substrate was 110 bp long, but that on shorter substrates the cutting pattern was changed to that predicted for the activity of a 3′-5′ exonuclease. Our results suggest that SbcCD processes hairpin and linear dsDNA ends with this novel DNA end-dependent binary endonuclease activity in response to substrate length rather than using previously reported activities. We propose a model for this mode of nuclease action, which provides new insight into SbcCD activity at a dsDNA end.

INTRODUCTION

The Mre11/Rad50 complex (composed of Mre11–Rad50-Nbs1 (MRN) or Mre11–Rad50-Xrs2 in eukaryotes, Mre11-Rad50 in archaea, SbcD-SbcC in bacteria and gp46-gp47 in bacteriophages) is known to be involved in a variety of cellular processes of genome maintenance such as DNA double-strand break (DSB) repair, telomere maintenance, replication fork stabilization and meiotic recombination (1–3). It plays various roles in these processes, and the roles in DSB repair are well characterized. The Mre11/Rad50 complex is essential for detecting DSBs, activating the DNA damage checkpoint and starting DNA end resection for homologous recombination. The core structure of this complex is well-conserved among species: the SMC family protein Rad50/SbcC dimer forms a characteristic V-shape structure with long coiled-coil arms, with one molecule of Mre11/SbcD nuclease attached to each arm, in a heterotetrameric complex ($Rad50_2/Mre11_2$ or $SbcC_2/D_2$) (4,5). The Rad50/SbcC dimer has the Walker A, B and signature motifs associated with ATPase activity, while Mre11/SbcD has phosphoesterase motifs responsible for nuclease activity. The bacterial and archaeal Mre11/Rad50 heterotetrameric complex is known to have a Mn^{2+} and adenosine triphosphate (ATP)-dependent 3′-5′ exonuclease activity and ATP-independent ssDNA endonuclease activity (6–10). Human Mre11 is reported to have ATP-independent 3′-5′ exonuclease activity and its activity was enhanced by complex formation with Rad50 (11). Human MRN complex possesses ATP-dependent endonuclease activity on hairpin-structured DNA (12). A recent study has shown that the yeast Mre11–Rad50-Xrs2 complex possesses ATP-independent 3′-5′ exonuclease activity and ATP-dependent endonuclease activity, which incises one strand of dsDNA endonucleolytically when stimulated by Sae2, and this incision is thought to initiate the 5′-3′ resection during DSB repair (13).

One of the activities of the $SbcC_2/D_2$ complex (SbcCD) in *Escherichia coli* is to process DNA hairpin structures formed at inverted repeats (14,15). A long inverted repeat (>150–200 bp) in a plasmid or phage is very poorly replicated and can be stably propagated only in *sbcCD*-deficient cells (16,17). Single-stranded DNA containing an inverted-repeat sequence can form a hairpin-like structure by intra-strand base pairing between reverse complement repeats. Biochemical study of *E. coli* SbcCD demonstrated that it has an ATP-dependent hairpin-opening activity that is conserved among species as other activities are. SbcCD introduces a nick at the stem-loop junction of a hairpin and continues cleaving one strand with its 3′-5′ exonuclease activity (8,11).

Inverted repeats are found abundantly in both eukaryotic and prokaryotic genomes, and long stretches of them can be hotspots of DSB formation. The Mre11/Rad50 complex has been proposed to be involved in DSB formation mediated by inverted repeats (16,18,19). Previous work analyzing chromosomes having 246-bp-long inverted repeats with a 24-bp spacer has suggested that SbcCD cleaves a single-strand hairpin structure formed at the inverted repeat by

*To whom correspondence should be addressed. Tel: + 81 743 72 5494; Fax: + 81 743 72 5499; Email: furukori@bs.naist.jp

progression of the replication fork (15). On the other hand, hairpin DNA has also been proposed to be formed during DNA repair. A broken chromosome end near inverted repeats might be capped by a hairpin structure during DSB repair. In cells without SbcCD and the recombination protein RecA, the presence of a 246-bp inverted repeat induced inverted chromosome duplications (20). It is proposed that SbcCD opens the hairpin-capped end up for homologous recombination to prevent a gross chromosomal rearrangement.

Inverted repeats can form another secondary structure called cruciform DNA, which is composed of two hairpins facing each other (18). In eukaryotes inverted repeats can extrude in a cruciform structure and be cleaved by a nuclease (21). In prokaryotes, on the other hand, cruciform extrusion and subsequent nuclease digestion is not evident, as the Holliday junction resolvase RuvABC is not involved in the inverted-repeat propagation in *E. coli*. A recent study by Leach *et al*. showed that SbcCD cleaves both leading- and lagging-strand at a perfect palindrome *in vivo* (22), but it is not yet clear whether SbcCD cleaves a cruciform or two hairpins individually formed on both strands at the fork. Here we have tested whether SbcCD cleaves cruciform DNA composed of two long hairpins formed at 246-bp inverted repeats in a negatively supercoiled plasmid. We have observed that SbcCD cleaved the cruciform DNA with unexpected cleavage patterns, repeatedly cleaving both strands of the cruciform stem at ∼10-bp intervals. Interestingly, we found that this cleavage was not dependent on the four-way structure of the cruciform; rather, it depended on the presence of a DNA end and on the length of the dsDNA. When the substrate dsDNA was long (110 bp), SbcCD cleaved both linear DNA and the dsDNA stem of a long hairpin molecule. We propose a model for the actions of SbcCD at the end of linear-shaped DNA and for SbcCD-mediated cleavage of hairpin DNA formed by a long inverted repeat.

MATERIALS AND METHODS

DNA substrates

Plasmid DNA. An inverted repeat-containing plasmid was constructed from pMOL7 by inserting the inverted-repeat fragment of pLacD1-pal246 between NsiI and ClaI sites (23,24). The resulting plasmid pIR246 contains 111-bp inverted repeats separated by a 24-bp spacer. The control plasmid pCNS was constructed from pIR246 by disordering the sequence of one of the 111-bp repeat units. These plasmids were purified from *E. coli* MK9200 *sbcC*201 *phoR*::Tn10 *tus*::Km using the Triton-lysis method (25). The supercoiled plasmid was then purified using a gel extraction method (23,26). The cruciform was extruded by heat-treatment at 80°C for 20 min in TE-NaCl (1 mM Tris–HCl pH 7.5, 0.1 mM ethylenediaminetetraacetic acid (EDTA), 100 mM NaCl) and cooling on ice.

244-mer hairpin DNA. A long hairpin substrate HP244 was prepared from pIR246. By BbsI and BsaI cleavages, inverted-repeat containing fragments (240 bp) were cut out and purified by the gel extraction kit (QIAGEN). The resulting hairpin DNA formed during the purification had a 110-bp stem with a 4-nt 5′-overhang (5′-AATT-3′). Klenow fragment (New England Biolabs) was used to fill in the overhang to make a blunt end. [α-^{32}P]dATP or dTTP (Perkin Elmer, 800 Ci mmol^{-1}) was used for 3′-end labeling, and T4 polynucleotide kinase (Toyobo) and [γ-^{32}P]ATP (Perkin Elmer, 3000 Ci mmol^{-1}) were used for 5′-end labeling.

Synthetic oligonucleotides. Synthetic oligonucleotides were purchased from FASMAC Co., Ltd. A set of oligonucleotides was incubated at 80°C for 10 min and then slowly cooled overnight to form dsDNA. Filling in and labeling of 5′- and 3′-termini were carried out in a way similar to the case of HP244. 110F: 5′-AATTCATTTCAGCATTTATTGGTTGTATGAGAGT AGATAGAAA AAGACAACTCTGGCTTGAAGCTAT CAAAAAACTAAGTAGTGATGAAAACTTTTCAA ATATGGAACTC (110-nt), 110R: 5′-GAGTTCCATA TTTGAAAAGTTTTCATCACTACTTAGTTTTTTGA TAGCTTCAAGCCAGAGTTGTCTTTTTCTATCTAC TCTCATACAACCAATAAATGCTGAAATG (106-nt), 27F: 5′-AATTCATTTCAGCATTTATTGGTTGTA (27-nt), 27R: 5′-TACAACCAATAAATGCTGAAATG (23-nt). Unlabeled synthetic oligonucleotides were prepared in a way similar to labeled synthetic oligonucleotides, except that the filling of 3′ termini by Klenow fragment was carried out with unlabeled dATP and dTTP.

Substrates bound on streptavidin magnetic beads. The 5′-overhang of each substrate was filled in using Klenow fragment in the presence of Biotin-11-dUTP (Thermo Scientific). The biotin-labeled substrates were then coupled with streptavidin magnetic beads (Dynabeads M-280 Streptavidin, Invitrogen) for 15 min at 25°C in a buffer containing 5 mM Tris–HCl, pH 7.5, 0.5 mM EDTA, pH 8.0 and 1 M NaCl.

DNA ladder markers for sequencing gel electrophoresis. DNA ladder markers were prepared using AmpliTaq DNA polymerase Stoffel fragment, dNTP, ddNTP, 5′-^{32}P-labeled primer and control plasmid pCNS by the Sanger sequencing method. The length of laddering DNA marker was used to estimate the length of a cleavage product.

Proteins

Wild-type SbcCD protein complex was overexpressed and purified from *E. coli* DL776 containing SbcCD-overexpressing plasmid pDL761 as described previously with minor modifications (7). Briefly, cell extracts were prepared using lysis buffer (50 mM Tris–HCl, pH 7.5, 1 mM EDTA, 50 mM NaCl, 10 mM β–mercaptoethanol, 10% (w/v) sucrose, 1 mM phenylmethylsulfonyl fluoride) by sonication followed by polyethyleneimine precipitation. SbcCD in the supernatant fraction was purified by 5 ml HiTrap DEAE (GE Healthcare), ammonium precipitation, Superose 6 HR 10/30 (Amersham) and Mono Q HR 5/5 (Amersham) as described. The peak fraction of SbcCD was dialyzed against buffer A (50 mM Tris–HCl, pH 7.5, 1 mM EDTA, 50 mM NaCl, 10 mM β–mercaptoethanol, 10% (v/v) glycerol), aliquotted, frozen in liquid nitrogen and stored at −80°C.

Mutant SbcCD H84N-expression plasmid was constructed from pDL761. Polymerase chain reaction (PCR)

primers were used to amplify DNA fragments with H84N mutation (1F: 5′-GGCAGGAAACAATGACTCGGTC, 1R: 5′-TTATTTCACTGCAAACGTACTTTCC). The rest of region was also PCR amplified (2F: 5′-GGAAAGTACGTTTGCAGTGAAATAA, 2R: 5′-GACCGAGTCATTGTTTCCTGCC) and two fragments were then joined together using an In-Fusion Advantage PCR cloning Kit (Clontech). The resulting plasmid pTrc99A-SbcCD-H84N was confirmed by sequencing, transformed into DL733 JM83 *sbcCD*::Km and used for purification of the mutant type of SbcCD in the way described above for the wild-type SbcCD. Note that the protein elution profiles of wild-type and of mutant SbcCD were similar in each of the purification steps.

Nuclease assays

Standard nuclease assay for pIR246 or pCNS was performed as described (7,8). Briefly, the assay was carried out in a reaction mixture (10 μl) containing 25 mM Tris–HCl, pH 7.5, 2% (v/v) glycerol, 100 μg ml^{-1} BSA, 1.25 mM dithiothreitol (DTT), 5 mM $MnCl_2$ and 1 mM adenosine triphosphate (ATP), 32.5 fmol of plasmid DNA (3.25 nM) and 300 ng protein (92 nM as $SbcC_2/D_2$ heterotetramer), unless indicated otherwise in the figure legends. The reaction mixtures were incubated at 37°C for the indicated time and reactions were stopped by adding an equal volume of 50 mM EDTA. The products were then purified by phenol/chloroform extraction and ethanol precipitation.

Standard assay conditions for hairpin and dsDNA substrates were identical to those for pIR246, except that 1.5 nM radiolabeled DNA and either 10 ng (1.5 nM) or 62.45 ng (9.6 nM) of protein were incubated in the 20-μl reaction mixture, as described in the figure legends. The assays shown in Figures 4 and 5 were carried out in this way but using 3′-biotinylated DNA substrates attached to streptavidin magnetic beads. After stopping the reaction by adding 50 mM EDTA, the products were separated into the supernatant and pellet fractions using the magnetic stand. Purified products were analyzed by denaturing or non-denaturing polyacrylamide gel electrophoresis (PAGE) analysis.

For the experiments in Figure 6, standard nuclease assay for dsDNA substrates were carried out as above using 1.5 nM [5′-^{32}P]ds110 or ds27 (0.03 pmol) and 138 nM SbcCD (900 ng) in the 20-μl reaction mixture, except that increasing amounts of unlabeled ds110 DNA were added (0, 0.03, 0.1, 0.3, and 3 pmol (final concentrations of 0, 1.5, 5, 15 and 150 nM, respectively)). Resulting reaction mixtures contain 0.03, 0.06, 0.13, 0.33 and 3.03 pmol of DNA (both labeled and unlabeled, final concentrations of 1.5, 3, 6.5, 16.5 and 152 nM), respectively. Products after 20-min incubation were analyzed by denaturing PAGE as described in the 'Materials and Methods' section.

Products analysis

Agarose gel electrophoresis for pIR246 and pCNS. The purified products were separated into two parts, and one of them was digested with restriction enzyme as indicated in the figure legend. Purified products were separated by 1% agarose gel at 50 V for 1 h in 1xTAE buffer, stained with ethidium bromide and visualized by using a UV transilluminator (ATTO).

Southern blot analysis for pIR246 and pCNS. The nuclease assay products were digested with two restriction enzymes, AseI and NsiI, to produce a 354-bp fragment. Purified DNA was then divided into two equal volumes, separated by sequencing gel electrophoresis together with radiolabeled laddering markers, electrically transferred onto a Hybond N+ nylon membrane (GE healthcare) by using a Gene Sweep sequencing gel transfer unit (Hoefer Scientific). In Figure 1D and E, the membrane was cut into three pieces (marker, probe A (lanes 1–5) and probe C parts (lanes 6–10)), and two pieces were hybridized with 5′-^{32}P-labeled probes A (5′- GTGTGTCTCAATCGATAACCTTATTTTTGACGAGG) or C (5′- TAAGCTCAGTCACGACGTTGTAAAACGACG). Those membranes were together exposed to a phosphor-imaging plate, and the radioactive signal was visualized using a BAS-2500 phosphorimager system and analyzed using Image Gauge (FujiFilm). Saturated signals are shown as pink-colored in the image. The identical method was applied for detection using probe B (5′- ATCAGCCTCATTTCTAAATATGAA) but using the membrane once used for probe A.

Sequencing gel electrophoresis analysis (Denaturing PAGE analysis). The purified products were resuspended in a sample buffer (10 mM EDTA, pH 8.0, 98% formamide, 0.005% xylene cyanol, 0.005% bromophenol blue), preheated at 100°C for 5 min and subjected to a sequencing gel electrophoresis using a 10% denaturing polyacrylamide gel (8 M urea, 6.3 M formamide) and 1× Tris-borate-EDTA (TBE) buffer at 35 W for 1.5 h. Products were visualized by phosphor-imaging with or without Southern blotting. Major product sizes indicated in all images are estimated roughly by comparison with the DNA ladder markers.

Native polyacrylamide electrophoresis analysis (Non-denaturing PAGE analysis). Purified cleavage products were resuspended in DNA sample buffer (30 mM EDTA, pH 8.0, 30% glycerol, 0.03% bromophenol blue). Prior to the sample loading, some of samples were pre-heated at 100°C for 5 min and immediately cooled on ice. The samples were analyzed by 12% native polyacrylamide gel electrophoresis in 1× TBE buffer at 100 V for 3 h. Products were analyzed by phosphor-imaging using a BAS-2500 scanner (FujiFilm).

RESULTS

SbcCD cleaves a cruciform stem endonucleolytically using a binary endonuclease activity

The long inverted repeats (246 bp; two 111-bp repeats separated by a 24-bp spacer) in a 4.7-kb negatively supercoiled plasmid pIR246 were extruded in a cruciform structure by heat treatment but not on control cruciform-free plasmid pCNS (27) (Figure 1A, Supplementary Figure S1, compare S1A, lane 1, and S1B, lane 1). Cruciform extrusion was confirmed by using four-way DNA junction resolvase T7 endonuclease I (Supplementary Figure S2). The plasmids were

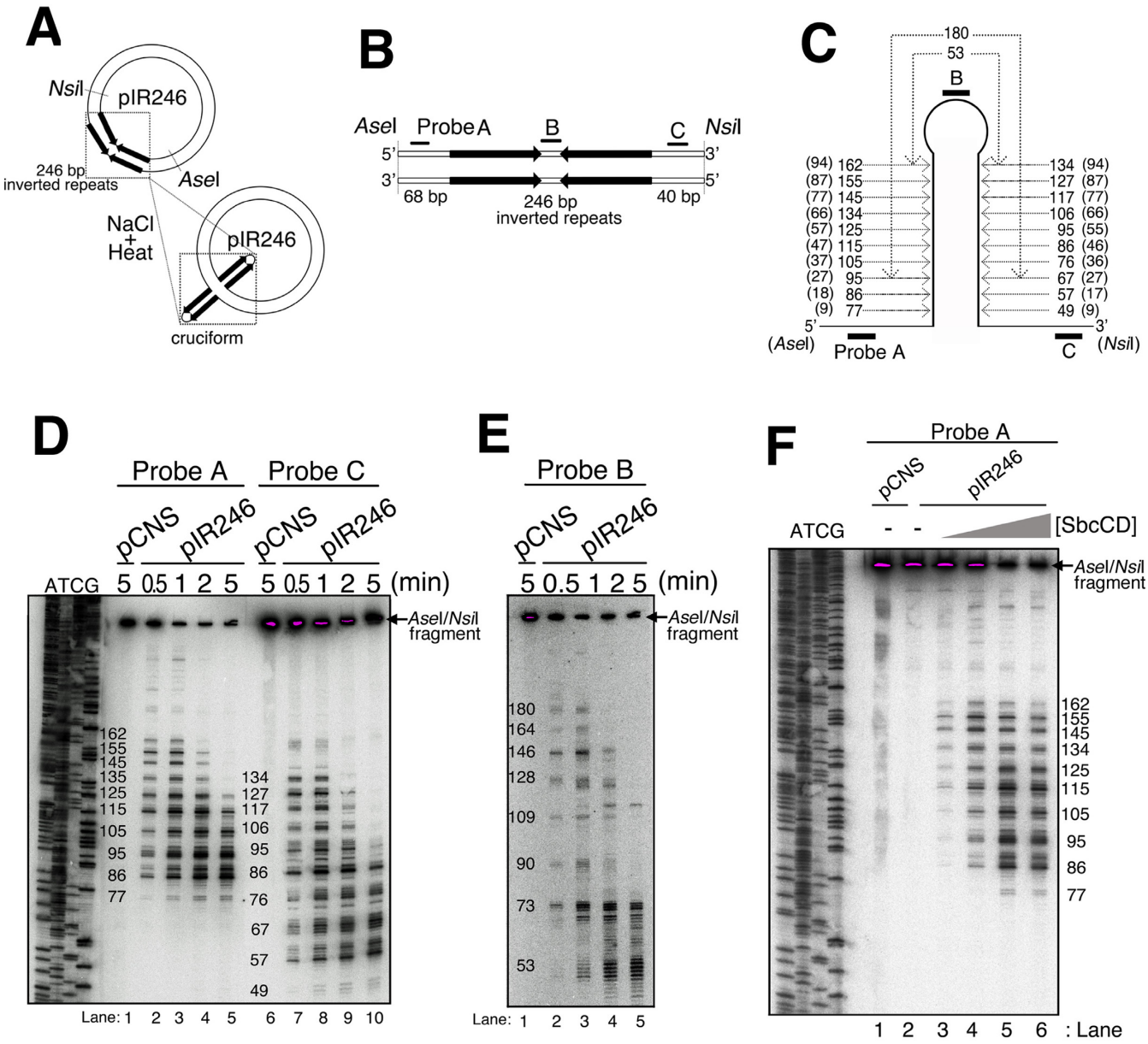

Figure 1. SbcCD cleaves the stem of the cruciform into 10-bp fragments with the novel nuclease activity. (**A**) Substrate DNA for SbcCD nuclease assay. The cruciform was extruded from 246-bp inverted repeats on supercoiled pIR246. (**B**) SbcCD-cleavage products of pIR246 and pCNS were digested by AseI/NsiI, separated on a sequencing gel (denaturing PAGE) and detected by Southern blotting. The locations of probes are indicated. The structure of control plasmid pCNS is shown in Supplementary Figure S1A. (**C**) Predicted major cleavage sites on a half of the cruciform. The estimated lengths of cleavage products are indicated in a drawing. The distances from the bottom of the cruciform are also indicated in brackets. (**D**) Nuclease assay was carried out with SbcCD (300 ng (92 nM)). A total of 3.25 nM of each plasmid was used in the nuclease assay. SbcCD-cleavage products separated by denaturing PAGE and detected by probes A and C at the indicated time points are shown. The inverted repeat-free plasmid pCNS was used as a control (lanes 1, 6). Size markers are indicated at the left side. Note that major product sizes indicated in all images are estimated roughly by comparison with the DNA ladder markers. (**E**) The products containing the loop between the repeats were detected by re-probing using probe B. (**F**) Nuclease assay was performed with increasing amounts of SbcCD (0, 30, 100, 300 and 900 ng (0, 9.2, 31, 92 and 275 nM, respectively), lanes 2–6). Products at 1-min incubation were separated by denaturing PAGE and detected by probe A.

incubated with SbcCD protein in the presence of ATP and manganese. The cruciform-extruded pIR246 was linearized by cleavage at the inverted repeats, while cruciform-free pCNS remained undigested (Supplementary Figure S1). It is reported that SbcCD introduces a nick at the stem/loop junction of synthetic oligonucleotide substrates forming short hairpin structures by its hairpin-opening activity and degrades one half of the stem by 3′-5′ exonuclease activity (cleavage products of a 56-mer hairpin HP56-CGAG (called as HP56 in this work) are shown in Supplementary Figure S6A) (8,28). To examine whether SbcCD cleaves the cruciform in a way similar to that of the hairpin substrate, the products were further treated with two restriction enzymes (NsiI/AseI) and subjected to sequencing gel electrophore-

sis (8M urea/6.3 M formamide denaturing PAGE, see 'Materials and Methods' section) followed by Southern blotting using specific probes to detect cleavage products (Figure 1B). Contrary to our expectations, laddering products with ∼10-nt intervals were detected with probes A and C (Figure 1C and D). SbcCD cleaved inverted repeats at multiple locations, not at a stem/loop junction as observed with a short hairpin. Cleavage sites detected by probe A were located within the 5′-side repeat unit, while those detected by probe C were within the 3′-side repeat unit. Cutting sites mapped on one repeat unit were in close proximity to those on the other unit when the inverted repeats formed a stem (Figure 1C). The longest products were produced by the cleavage at either ∼15 or 25 bp from the loop, but they became shorter when the incubation time or the SbcCD concentration was increased (Figure 1D and F). The cleavage ceased when the remaining stem was less than about 10–20-bp. These data show that the cleavage occurred repeatedly on the dsDNA stem of the cruciform. When probe B was used to detect cleavage products containing the 24-nt loop, laddering products with roughly 20-nt interval (with the sizes of ∼53 to 180 nt) were detected (Figure 1E). The longer products also became shorter depending on the incubation time. These data show that SbcCD cleaves the stem of a cruciform endonucleolytically by clipping DNA double strands coordinately. The initial cleavage sites seemed to occur with 10-bp interval at various locations on the entire stem.

This is not a usual endonuclease activity, because like an exonuclease it requires a dsDNA end (a hairpin-loop terminus in this case) to start cleavage and does not cleave a circular plasmid (Supplementary Figure S1A). Since SbcCD introduces nicks simultaneously on two strands of dsDNA, we call this novel dsDNA cleavage activity 'DNA end-dependent binary endonuclease' activity (binary endonuclease activity). Notably, Connelly *et al.* previously reported that SbcCD can remove a capping protein at the end of linear dsDNA by introducing nicks on two strands (29). This dsDNA endonuclease activity was observed on a protein-bound DNA end adjacent to the capping protein when the 3′-5′ exonuclease activity was restricted, and the authors speculated that SbcCD initially binds at an internal region of dsDNA and introduces DSB upon encountering a blocked terminus. Our new results suggest that under conditions where the 3′-5′ exonuclease activity of the enzyme is permitted, dsDNA cleavage from the vicinity of an end occurs repeatedly without the addition of a capping protein.

SbcCD cleaves the stem of a hairpin DNA and a linear dsDNA by binary endonuclease activity

To test whether the binary endonuclease activity is observed only when a long hairpin is in a four-way structure on a plasmid, a long hairpin substrate HP244 (244 mer; 110-bp stem and 24-nt loop) was prepared by cutting out the DNA fragment from pIR246. The SbcCD cleavage of each strand of the dsDNA was analyzed using a 5′- or 3′-radiolabeled substrate ([5′-^{32}P]-HP244 or [3′-^{32}P]-HP244) (Figure 2A). SbcCD was able to digest HP244 in a way similar to that observed with the cruciform extruded plasmid DNA (Figure 2B–D). Cleavage of dsDNA by SbcCD started at ∼15 nt from the loop and repeatedly occurred with about 10-nt intervals on both strands in close proximity (Figure 2B and D), indicating that the binary endonuclease activity is effective on a long hairpin DNA and does not require the four-way junction structure of cruciform DNA. The 5′-labeled strands were degraded to 12 nt after incubation with SbcCD (Figure 2C, lane 8). Shorter products with 1-nt laddering were also observed, suggesting that the binary endonuclease-products are likely to be further degraded by 3′-5′ exonuclease activity.

We designed and purified a nuclease-deficient mutant protein SbcCD H84N (Figure 3A). It has a single amino-acid substitution in the nuclease motif III of SbcD, which is known to disrupt all nuclease activities of Mre11/Rad50 complex (*Pyrococcus furiosus* H85S, *Saccharomyces cerevisiae* H125N, murine H129N and human H129D) (30–33). SbcCD H84N did not digest either linear dsDNA or cruciform-extruded pIR246 (Figure 3B and C). This mutant SbcCD enzyme also did not cleave HP244 by the binary endonuclease activity (Figure 3D). The 10-bp laddering products were not observed with the mutant enzyme, although a very weak nicking activity, which could be a contaminant nuclease activity or a residual activity of SbcCD H84N, was observed (compare lanes 2–6 and lanes 8–11). The result clearly demonstrates that both the 3′-5′ exonuclease activity and the binary endonuclease activity share the same catalytic center of SbcD. The binary endonuclease activity was observed in the presence of manganese, which could not be substituted by magnesium (Supplementary Figure S3A). This activity was not observed in the absence of ATP and was enhanced by ATP hydrolysis (Figure 3E). It is reported that Mg^{2+} supports Rad50's ATP hydrolysis (34). When both manganese and magnesium salts were added to the reaction, the activity slightly increased with increasing concentration of Mg^{2+}, also suggesting that ATP hydrolysis stimulates the binary endonuclease activity (Supplementary Figure S3B). The addition of Zn^{2+} or NaCl did not significantly alter the product pattern of the activity in the presence of manganese (Supplemental Figure S3A and C).

It has been accepted widely that the predominant activity of the Mre11/Rad50 complex is 3′-5′ exonuclease activity on linear dsDNA (11,28). However we have observed a similar 10-bp laddering pattern of DNA cleavage when a synthetic linear dsDNA substrate (ds110) identical to the stem DNA of HP244 (Figure 2E) was incubated with SbcCD (compare Figure 2B, D, F and G. Cutting sites are shown in Supplementary Figure S4A). We have also observed characteristic 10-bp interval cleavages of the 5′-terminal strand at the end region of a 4.7-kb linear dsDNA with little or no sequence dependence (Figure 2H and Supplementary Figure S4B). Therefore, SbcCD acts as a binary endonuclease on linear DNA as well as on the stem of a cruciform structure or of a DNA hairpin substrate.

SbcCD cleaves linear dsDNA by binary endonuclease activity depending on the substrate length and [SbcCD]:[DNA] ratio

Although SbcCD has 3′-5′ exonuclease and binary endonuclease activities, both of which depend on ATP, the requirements for the latter activity have not been investigated. As

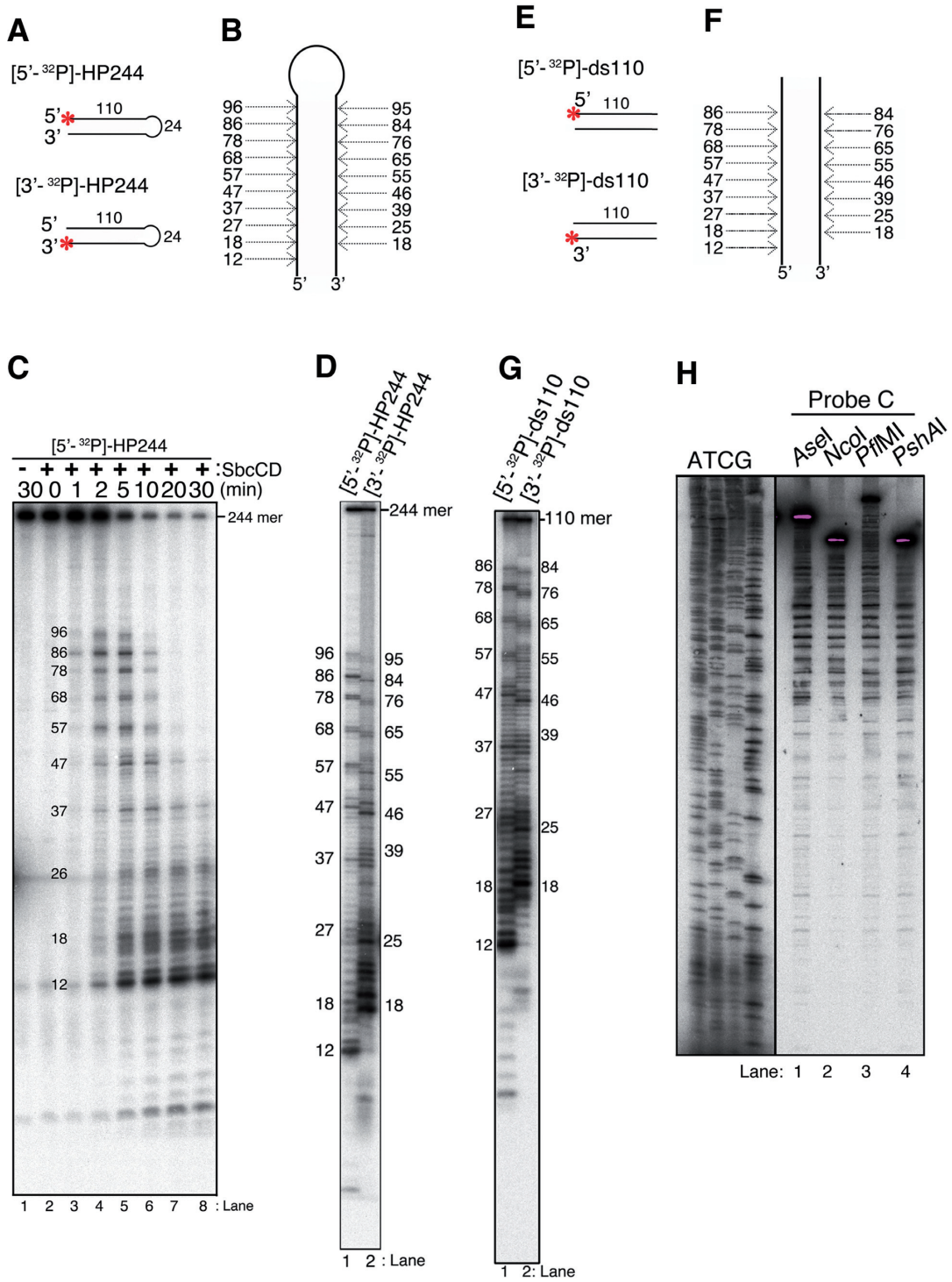

Figure 2. SbcCD cleaves a long hairpin or linear dsDNA with its binary endonuclease activity. (**A**) Hairpin DNA (244-mer) prepared from pIR246. Either the 5′ or 3′ terminus of each substrate was ^{32}P-labeled (indicated as a red asterisk). (**B**) Major cutting sites for HP244 are shown within a schematic drawing. (**C**) Nuclease assay was carried out with SbcCD (10 ng (1.5 nM)) and [5′-^{32}P]-HP244 (1.5 nM) and products at increasing incubation times separated by denaturing PAGE are shown. (**D**) Substrate DNA were incubated with SbcCD (10 ng (1.5 nM)) in the standard assay condition. Products were separated by denaturing PAGE. Comparison of 5′- and 3′-labeled hairpin substrates are shown. (**E**) Linear dsDNA substrate (110-bp) ^{32}P-labeled at either the 5′ or 3′ end. (**F**) Major cutting sites for ds110 are shown. (**G**) Product comparison of 5′- and 3′-labeled linear-dsDNA substrates on denaturing PAGE are shown. (**H**) SbcCD cleaves the end of a linearized 4.7-kb plasmid with its binary endonuclease activity. Control 4.7-kb plasmid pCNS (inverted-repeat free) was linearized by the restriction enzyme as indicated in the figure. Linearized plasmid with various shapes of the end (2- or 4-nt overhang 5′-sticky, or 3-nt overhang 3′- sticky or blunt ends) was used as the substrate for SbcCD nuclease assay (SbcCD 900 ng (275 nM), DNA 3.25 nM). The products at 1-min incubation were purified, digested by NsiI, separated by a denaturing PAGE and detected by Southern blotting using probe C as in Figure 1. Cleavage in the 5′- to 3′-direction was observed. Detailed cutting sites are shown in Supplementary Figure S4B. Size markers are indicated on the left.

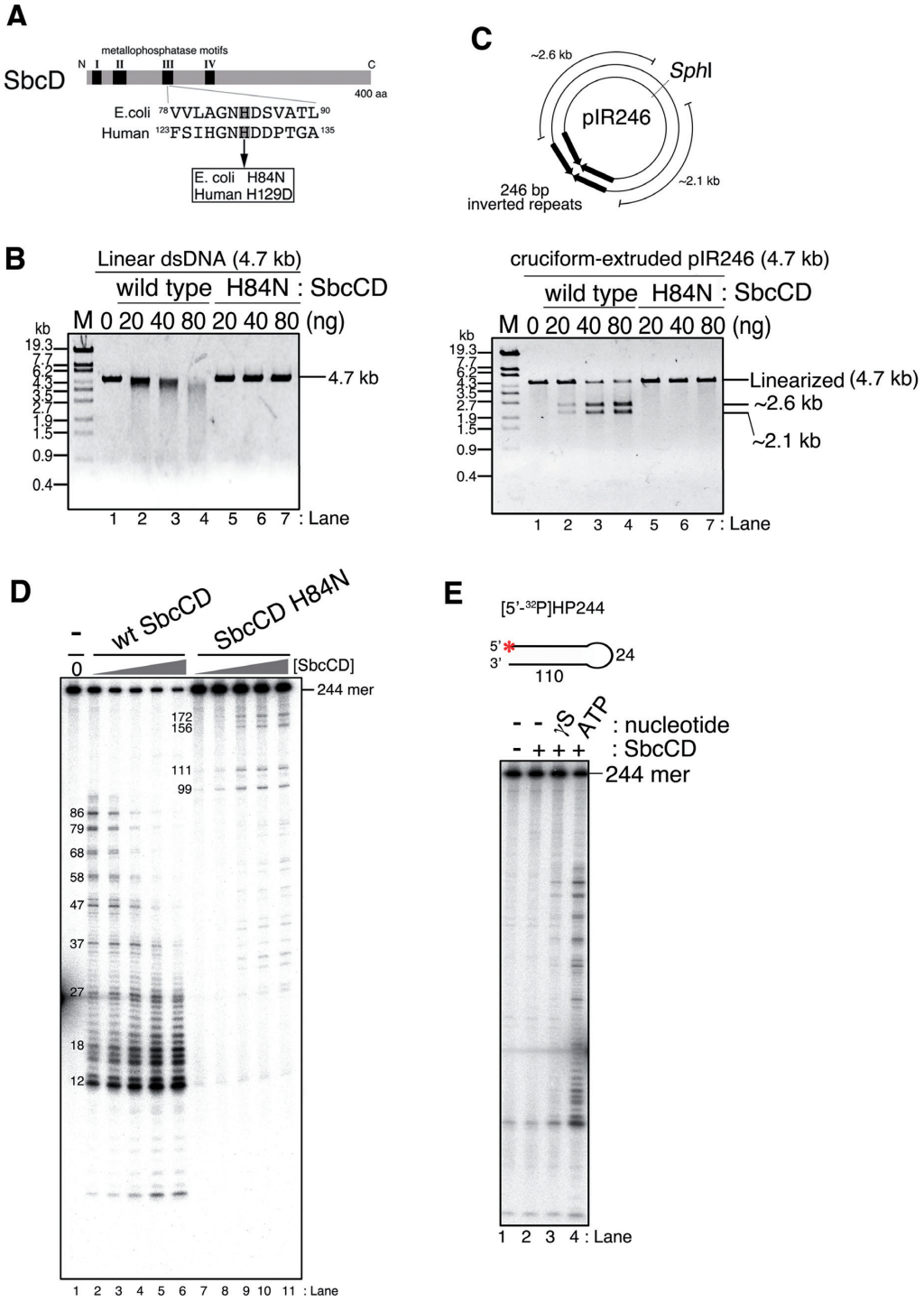

Figure 3. An amino acid substitution (H84N) in motif III of SbcD abolishes all nuclease activities, including the binary endonuclease activity. (**A**) Schematic drawing of SbcD. Substitution of asparagine for a conserved histidine in nuclease motif III was predicted to inactivate nuclease activities of SbcD. Comparable sequence of human Mre11 is indicated. (**B**) Nuclease activity of increasing amounts (0, 20, 40 and 80 ng (0, 6.1, 12 and 24 nM, respectively)) of wild-type SbcCD (lanes 1–4) or mutant SbcCD (lane 5–7) were tested using linearized pCNS (4.7 kb) as a substrate (3.25 nM). Products of 20-min incubation were analyzed by agarose gel electrophoresis. (**C**) Upper: schematic diagram showing the location of restriction site and predicted cleavage products of pIR246. Lower: nuclease assay was carried out under the same conditions as in (B) except that the cruciform-extruded, circular pIR246 was used as a substrate as in Supplementary Figure S1B. After nuclease assay completed, purified cleavage products were digested by SphI and analyzed by agarose gel electrophoresis. The distances between the inverted repeat and SphI site were ∼2.1 and 2.6 kb. (**D**) Nuclease assay was carried out using increasing amounts of wild-type SbcCD or nuclease-deficient mutant SbcCD H84N (0, 5, 10, 20, 40, 80 ng (0, 0.75, 1.5, 3.1, 6.1 and 12 nM, respectively)) with 20-min incubation. [5′-^{32}P]-HP244 was used as a substrate. Products were analyzed by denaturing PAGE. (**E**) The binary endonuclease activity of SbcCD is ATP-dependent and is stimulated by ATP hydrolysis. SbcCD nuclease assay with [5′-^{32}P]-HP244 was carried out in the standard condition, except that ATP was omitted or substituted by the non-hydrolyzable analog ATP-γ-S as indicated. The products after 5-min incubation were analyzed by denaturing PAGE. Substrate DNA (244-mer hairpin) is shown on the image. Location of 5'-^{32}P-label is indicated (a red asterisk).

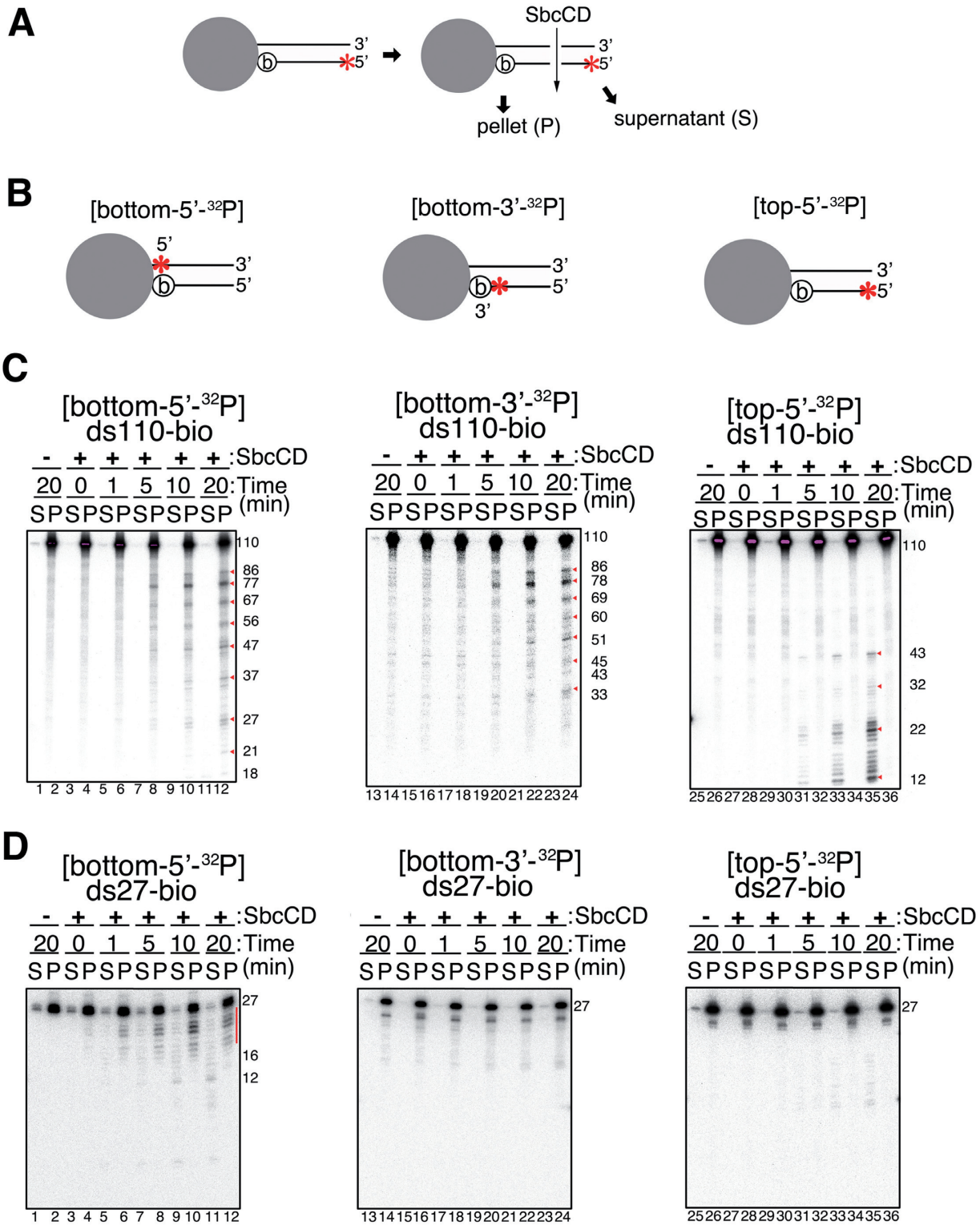

Figure 4. The binary endonuclease activity is detected with long dsDNA substrates, while only 3′-5′ exonuclease activity is observed with short dsDNA substrates. (**A**) Schematic diagram for the assay. One end of dsDNA was 3′-biotinylated ('b' in a circle) and blocked by streptavidin beads (large gray sphere). Products cleaved out from the beads were collected in the supernatant fraction (S), while those bound on beads were recovered in the pellet fraction (P). Products in each fraction were analyzed by denaturing PAGE. (**B**) Substrate DNA used for nuclease assays. Locations of 5′- or 3′-^{32}P-label are indicated (red asterisks). Three types of substrate were prepared for either 110- or 27-bp dsDNA. (**C**) Nuclease assay for SbcCD (10 ng (1.5 nM)) was carried out with each of three types of 110-bp substrate (1.5 nM). On 110-bp dsDNA, cleavages occurred in both the 3′-5′ (left panel, lane 12) and 5′-3′ directions (middle panel, lane 24). Cleaved DNA was released into the supernatant (right panel, lane 35). SbcCD-specific cleavage sites are shown as red arrowheads. (**D**) Nuclease assay for SbcCD (62.45 ng (9.6 nM)) was carried out with each of three types of 27-bp substrate (1.5 nM). Only the 3′-5′ exonuclease activity was observed (marked as a red line. left panel, lane 12).

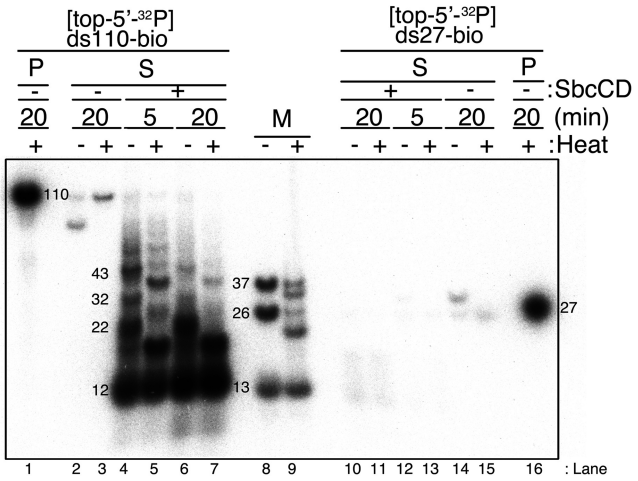

Figure 5. The binary endonuclease activity produces short double-stranded DNA fragments from 110-bp substrate but not from 27-bp substrate. Nuclease assay for SbcCD (62.45 ng (9.6 nM)) was performed with 1.5 nM bead-bound, linear 110- or 27-bp substrate 5′-radiolabeled at the top, as in Figure 4C and D, right panel. The ^{32}P-labeled cleavage products released into the supernatant at 5 or 20 min were analyzed by native (non-denaturing) PAGE with or without heat treatment as indicated. The products obtained from 110-bp substrates were double-stranded (lanes 4–7). Size marker dsDNAs (37, 26 and 13 bp) with or without heat treatment were subjected to the same non-denaturing PAGE as a control (lanes 8 and 9).

many of the DNA substrates used in previous studies have been shorter than those used here, we hypothesized that the binary endonuclease activity might become detectable only when the dsDNA substrate was longer than a particular size. To test the idea that the length of substrate may modulate the activity of SbcCD, we analyzed SbcCD action intensively on two different sizes of substrate (ds110 and ds27 (110- and 27-bp linear dsDNA)), which correspond to the stems of HP244 and HP56, respectively. Although the endonucleolytic action of SbcCD cannot be totally restricted by the terminal blockage, the 3′-end of one strand was biotin-conjugated (ds110-bio and ds27-bio) and attached to streptavidin magnetic beads to protect one end from the exonucleolytic action of SbcCD (Figure 4A). Three-types of ^{32}P-radiolabeled substrates were prepared for both ds110 and ds27; 5′- or 3′- labeled on the bead-side end or 5′- labeled on the other side end. These substrates were denoted bottom-5′-^{32}P, bottom-3′-^{32}P and top-5′-^{32}P, respectively (Figure 4B). As digestion of the shorter substrate was difficult to detect with a low concentration of enzyme, an increased amount of SbcCD was used for ds27 (ds110; 1.5 nM, ds27; 9.6 nM as $SbcC_2/D_2$ heterotetramer). After incubation with SbcCD for the times indicated, the DNA released into the supernatant (S) and that which remained attached to the beads (P) were fractionated and analyzed (Figure 4A, C and D). As a consequence of binary endonuclease action, laddering products with 10-nt interval were observed in the bead fractions of [bottom-5′-^{32}P]ds110-bio and [bottom-3′-^{32}P]ds110-bio (Figure 4C, left and middle panel, lanes 12 and 24, products are marked as red arrowheads). Accordingly, increasing amounts of shorter laddering products were recovered in the supernatant fraction with [top-5′-^{32}P]ds110-bio (Figure 4C, right panel, lane 35). The shortest one (∼12 nt) and the next-shortest one (∼22 nt) were major products, and some ∼32- and ∼43-nt products were also detected. In contrast, a 1-nt laddering pattern was detected in the bead fraction of [bottom-5′-^{32}P]ds27-bio (Figure 4D, left panel, lane 12, marked as a red line), while such a cleavage pattern was not observed with [bottom-3′-^{32}P]ds27-bio (Figure 4D, compare lanes 12 and 24). Furthermore, just a trace amount of degraded DNA was detected in the supernatant of [top-5′-^{32}P]ds27-bio (Figure 4D, right panel, lane 35). These degradation products are possibly 5′-labeled ds27 that had detached spontaneously and was cleaved by the 3′-5′ exonuclease activity of SbcCD. These results indicate that SbcCD starts cleavage of the 110-bp substrate by binary endonuclease activity, while on the 27-bp dsDNA it acts exclusively as a 3′-5′ exonuclease.

To demonstrate that the cleaved products of ds110-bio are double-stranded, the products in the supernatant fractions were analyzed by non-denaturing PAGE (Figure 5). A heat treatment denatured dsDNA to ssDNA and produced faster migrating species in the non-denaturing PAGE, as observed with the 26- and 37-bp labeled dsDNA size markers. A 13-bp marker DNA showed no significant mobility difference produced by the heat treatment in this analysis (Figure 5, lanes 8 and 9). The DNA molecules released from [top-5′-^{32}P]ds110-bio and recovered in the supernatant fractions were of particular sizes, corresponding to the ∼12-, 22-, 32- and 43-bp products observed in Figure 4C. The heat treatment of these DNA fragments enhanced their migration in the non-denaturing PAGE (Figure 5, compare lanes 4 and 6 and lanes 5 and 7), implying that these cleavage products were double-stranded. Such double-stranded products were not detected with [top-5′-^{32}P]ds27-bio (Figure 5, lanes 10–13). In contrast, we observed that SbcCD produced short dsDNA fragments from a 40-bp dsDNA substrate (Supplementary Figure S5). We speculate that the threshold length for the binary endonuclease activity lies between 27 and 40 bp. These data also show that SbcCD becomes active as a binary endonuclease on dsDNA fragments that are longer than this threshold length.

We found that SbcCD's activities on a long dsDNA also depended on the concentrations of SbcCD and DNA. At lower concentration of SbcCD (0.77–1.5 nM, [SbcCD]:[DNA] = 0.5:1–1:1, Figure 6A and B, lanes 4 and 5), the characteristic 10-bp laddering products were clearly observed with ds110 while little activity was detected on ds27. Increasing concentration of SbcCD resulted in the decrease of remaining undigested ds27, suggesting that the cleavage by 3′-5′ exonuclease activity increased as expected (Figure 6B). Interestingly, with ds110, cleavage by the binary endonuclease activity was significantly inhibited at high concentrations of SbcCD (46 and 138 nM, [SbcCD]:[DNA] = 30:1 and 90:1, Figure 6A, lanes 9 and 10). The same phenomenon was observed with the hairpin substrate HP244 but not with HP56 (Supplementary Figure S6B). When increasing concentrations of unlabeled substrate DNA were added to the reaction, even at a high concentrations of SbcCD (138 nM), the nuclease activities were gradually restored (Figure 6C, lanes 3–5). The 10-bp ladder-

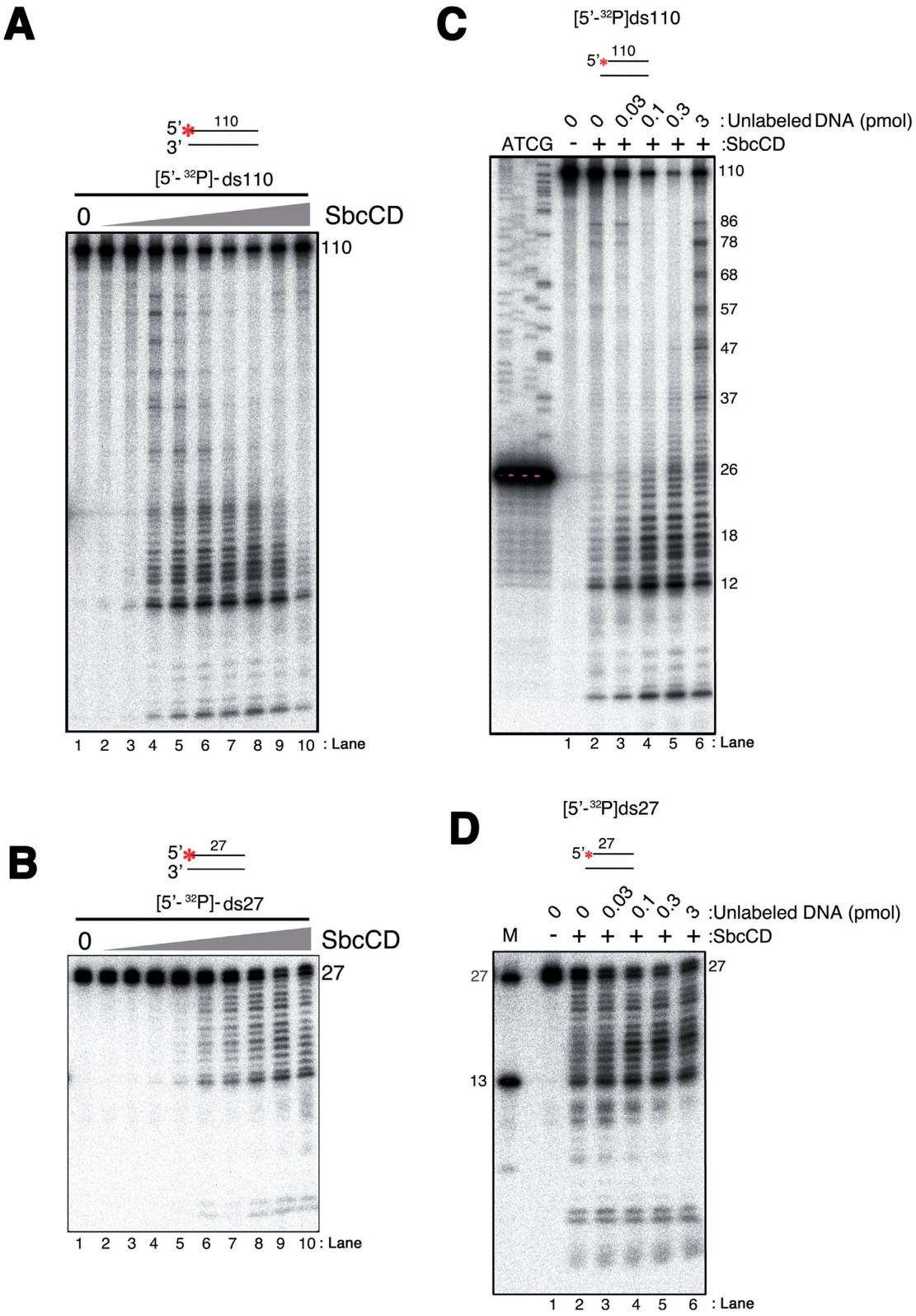

Figure 6. DNA length-dependent nuclease actions of SbcCD also depended on the ratio of concentrations of SbcCD and of DNA. (**A** and **B**) SbcCD titration assay. Standard nuclease assay were carried out using 1.5 nM [5′-^{32}P]ds110 (A) or 1.5 nM [5′-^{32}P]ds27 (B) in the presence of increasing amount of SbcCD (0, 0.5, 1, 5, 10, 30, 60, 100, 300 and 900 ng (0, 0.077, 0.15, 0.77, 1.5, 4.6, 9.2, 15, 46 and 138 nM, respectively)). Products after 20 min of incubation were analyzed by denaturing PAGE. (**C** and **D**) Standard nuclease assay were carried out at high concentration of SbcCD (138 nM) using 1.5 nM [5′-^{32}P]ds110 (C) or 1.5 nM [5′-^{32}P]ds27 (D) as a substrate. In lanes 2–6, increasing amounts (0, 0.03, 0.1, 0.3 and 3 pmol) of unlabeled ds110 (C) or ds27 (D) were added. Resulting total DNA final concentrations are 1.5, 3, 6.5, 16.5 and 152 nM, respectively (lanes 2–6). Products after 20-min incubation were analyzed by denaturing PAGE. Substrate DNA are shown on the images. Location of 5'- ^{32}P-label is indicated (a red asterisk).

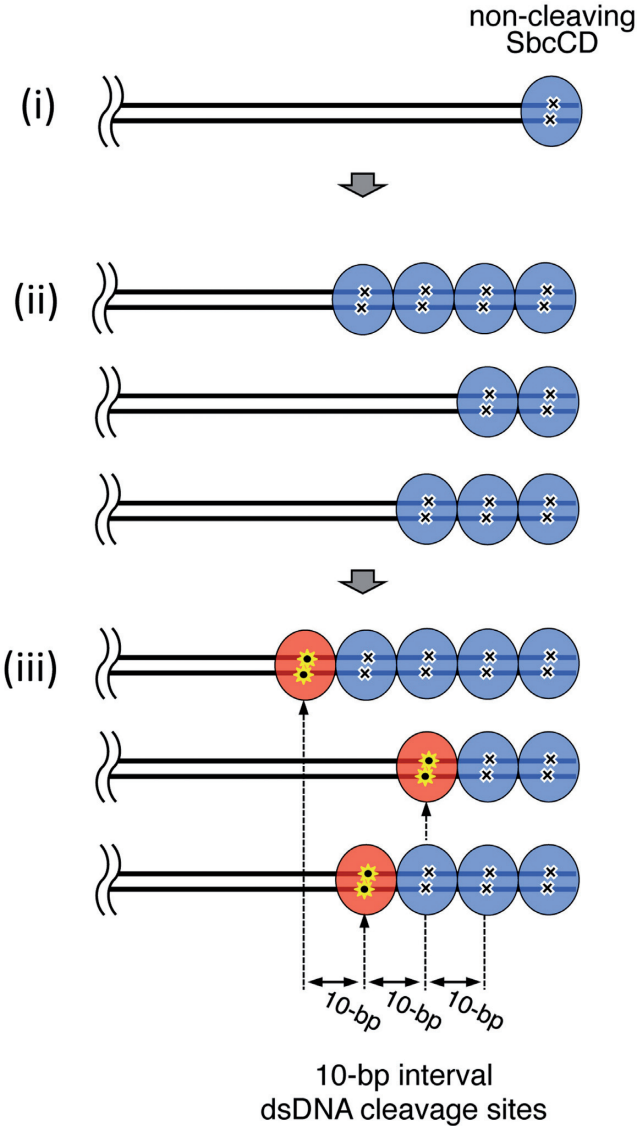

Figure 7. Hypothesis for binary endonuclease action of SbcCD. A non-cleaving SbcCD array may be formed on a DNA end prior to the nucleolytic action. (i) The terminal binding of one inactive SbcCD (blue oval, catalytic centers in the $SbcD_2$ are shown as black x-marks) blocks the DNA end. (ii) The tandem array of non-cleaving SbcCD is formed from the dsDNA end. (iii) SbcCD is activated as a binary endonuclease at various locations with 10-bp intervals (shown as a red oval with yellow stars). Depending on the number of terminal SbcCD complexes in the array of each substrate molecule (2–4 are shown in the model), the cleavage occurs at different positions, producing 10-bp (or multiple of 10-bp) dsDNA fragments from the DNA end.

ing products were again observed at a high concentration of DNA (the final concentration of total DNA is 152 nM, [SbcCD]:[DNA] = 0.9:1, lane 6). These results suggest that on a long dsDNA the nuclease action of SbcCD relates inversely to the SbcCD to DNA ratio.

DISCUSSION

We describe how SbcCD cleaves a long, linear-shaped dsDNA with or without a loop at the end. SbcCD cleaves dsDNA longer than ∼40 bp using a binary endonuclease activity, which produces 10-bp laddering products and depends on the presence of a DNA end or end-like structure. Furthermore, the end that activates the binary endonuclease activity can be present on a cruciform, hairpin or duplex DNA substrate demonstrating that neither the four-way junction of the cruciform (not present in the hairpin or the duplex DNA) nor the open double-stand end of the hairpin (not present in the cruciform) are required for activation.

The binary endonuclease activity of SbcCD depends on the length of dsDNA substrate. This length-dependence led us to hypothesize that SbcCD may have an affinity for dsDNA strands that leads to binary endonuclease activity when the same substrate also contains a DNA end. If SbcCD binds dsDNA strands, it will be loaded on dsDNA more easily the longer the dsDNA substrate becomes. Supporting this idea, the binary endonuclease activity was clearly observed at a very low concentration of SbcCD on long substrates, while the 3′-5′ exonuclease activity was not detected at the same concentrations (Figure 6A and B). By contrast we hypothesized that, when the dsDNA substrate was short, SbcCD would not be loaded to the internal ds part of the substrate but instead the enzyme in solution would interact directly with the DNA end and distributively cleave using its 3′-5′ exonuclease activity. The efficiency of 3′-5′ exonucleolytic cleavage of ds27 increases as the concentration of SbcCD is increased (Figure 6B), supporting the idea that the 3′-5′ exonuclase reaction is distributive.

By contrast with the concentration dependence of the 3′-5′ exonucleolytic cleavage of the short substrate, the binary endonuclease action on ds110 was strongly inhibited at high concentrations of SbcCD (Figure 6A and Supplemental Figure S6B). Interestingly, even at the high concentration of SbcCD (275 nM), the binary endonuclease activity was not inhibited when cruciform-extruded pIR246 (4.7 kb) was used as a substrate (Figure 1F, lane 6). The difference caused by the total substrate length may imply that SbcCD binds weakly on a long dsDNA strand as proposed earlier (29), in this case, the circular region of the plasmid (as well as to the extruded hairpin arms). This effect of the presence of extra dsDNA was shown to operate *in trans* when excess unlabeled linear ds110 substrate was added to a labeled ds110 cleavage reaction and stimulated binary endonuclease activity (Figure 6C). The binary endonuclease activity of SbcCD must be regulated in a complex manner that depends critically on the ratio of SbcCD to total dsDNA and to DNA ends. Clearly DNA ends are required as SbcCD not cleave the control plasmid pCNS (Supplemental Figure S1A).

Using a 4.7-kb linear dsDNA substrate, dsDNA cleavage was observed to occur from the vicinity of the end (Figure 2H), suggesting that the binary endonuclease activity is not only DNA end-dependent but is activated in the vicinity of the DNA end. Currently, how the DNA end activates the SbcCD binary endonuclease activity is unclear, but we have made several observations that have led us to propose a model that is consistent with the data. The observation that SbcCD preferentially cleaves a long dsDNA substrate by the binary endonuclease activity, not by the 3′-5′ exonuclease activity, even though an end that might be susceptible to the 3′-5′ exonuclease activity is present (Figure 4C)

suggests that SbcCD itself has an ability to protect the DNA end from its own exonucleolytic degradation when it works as a binary endonuclease. The protective action of SbcCD was more clearly observed when the [SbcCD]/[DNA] ratio was high (Figure 6 and Supplementary Figure S6). Both binary endonuclease and 3′-5′ exonuclease activities on the dsDNA stem were restricted, while ssDNA endonuclease activity was allowed to work on the ssDNA loop (Supplementary Figure S6B). The fact that the ratio between the enzyme and DNA greatly affected the cleavage/protective actions suggests that more than one molecule of SbcCD is involved in the reaction on a dsDNA substrate. These observations provide a possible explanation for the DNA end-dependency of the binary endonuclease activity (Figure 7). In this hypothesis, prior to the cleavage reaction, with a strong affinity or slow dissociation, SbcCD binds to the terminus of dsDNA without cleavage action and protects the end from other SbcCD molecules (Figure 7, (i)). Then, a dynamic tandem array of non-cleaving SbcCD is formed from the end (Figure 7, (ii)). When the concentration of SbcCD is too high compared to that of DNA, SbcCD may be overloaded on DNA and the SbcCD array may be extensively formed to cover the substrate. Connelly *et al.* previously proposed that SbcCD might translocate along dsDNA and cleave both strands when encountering a blocking protein (29). In our case, the terminal non-cleaving SbcCD array may stimulate the binary endonuclease activity when another SbcCD is loaded on the internal position of DNA encounters the terminal complex. What differentiates a cleaving from a non-cleaving SbcCD complex is currently unknown.

This hypothesis explains several of our key observations. SbcCD's binary endonuclease activity cleaves dsDNA at locations multiples of 10-bp away from the end. When a low concentration of SbcCD was used for a short-time incubation, and a large amount of undigested substrate remained in the reaction, not only the first cleavage site but also internal cleavage sites located multiples of 10 bp away from end were detected (Figure 2C, lane 4; Figure 4C, lane 8). This implies that even if SbcCD skips several cleavage sites, the cleavage occurs at the same locations on dsDNA with a distance of a multiple of 10-bp away from the end (Figure 1E, lane 2; Figure 5, lane 4). It is possible that the initial binding of inactive SbcCD at the end may stimulate the formation of an inactive SbcCD array by capping the array and this is followed by binary-endonuclease activation (Figure 7, (i–iii)). It has been reported that the size of the globular domain of SbcCD is ∼3.4 nm (8), which corresponds to the length of one helical turn (∼10.5 bp per turn in B-form dsDNA). Different numbers of terminal SbcCD complexes in the array may protect DNA with periodic sizes of multiples of 10-bp causing the characteristic 10-bp laddering products (Figure 7, (iii)). Although the existence of a non-cleaving SbcCD array at a DNA end has not been demonstrated in this work, the hypothesis provides reasonable explanations for the actions of SbcCD found in this study and is a target for future testing. A much simpler model, for example, one in which a single SbcCD processively cleaves dsDNA from the end, cannot explain why the binary endonuclease activity is DNA length- and [enzyme]/[DNA] ratio-dependent and how SbcCD produces 10-bp laddering products.

It is known that long inverted repeats cannot be propagated in *sbcCD*-proficient cells and are therefore not found in *E. coli* genome (14,17). *In vivo* data suggested that SbcCD cleaves a hairpin formed at long inverted repeats during DNA replication (15,22), but the molecular basis underlying the selection of long inverted repeats by SbcCD remains unclear. Findings described in this study may help us understand how SbcCD selectively works on hairpin structures formed at a long inverted repeats in cells if only the binary endonuclease activity of the enzyme is permitted *in vivo*. On the other hand, relatively short inverted repeats, palindromes and quasi-palindromes are scattered in the *E. coli* genome, and some of them are known to have important cellular functions (18). In *E. coli,* a powerful exonuclease RecBCD is thought to produce DNA with a 3′-overhang to repair a DSB by homologous recombination, but if a DSB occurs near an inverted repeat and a hairpin-capped DNA end is formed during the repair process, cellular exonucleases are not able to degrade it. Our results also showed that SbcCD removed a hairpin from linear-shaped dsDNA and produced a nearly blunt DNA end. SbcCD might be important to facilitate proper homologous recombination by removing the hairpin, preventing chromosomal rearrangements as previous *in vivo* work has suggested (20). Our findings suggest how SbcCD may act at a DNA end if linear-shaped dsDNA more than 27–40 bp long is formed during DNA replication and repair processes. If the binary endonuclease action found in this study is conserved in the eukaryotic Mre11/Rad50 complex, our findings may help explain the intricate actions of MRN complex in human cells.

SUPPLEMENTARY DATA

Supplementary Data are available at NAR Online.

FUNDING

Grants-in-Aid for Scientific Research KAKENHI [25840009 to A.F.; 25291077, 25131713 to H.M.] from the Japan Society for the Promotion of Science and the Ministry of Education, Culture, Sports, Science and Technology, Japan; UK Medical Research Council (MRC) (to D.R.F.L.). Funding for open access charge: Grants-in-Aid for Scientific Research KAKENHI from the Japan Society for the Promotion of Science and the Ministry of Education, Culture, Sports, Science and Technology, Japan [25840009 to A.F.].
Conflict of interest statement. None declared.

REFERENCES

1. Williams,G.J., Lees-Miller,S.P. and Tainer,J.A. (2010) Mre11-Rad50-Nbs1 conformations and the control of sensing, signaling, and effector responses at DNA double-strand breaks. *DNA Repair (Amst)*, **9**, 1299–1306.
2. Stracker,T.H. and Petrini,J.H. (2011) The MRE11 complex: starting from the ends. *Nat. Rev. Mol. Cell Biol.*, **12**, 90–103.
3. Paull,T.T. (2010) Making the best of the loose ends: Mre11/Rad50 complexes and Sae2 promote DNA double-strand break resection. *DNA Repair (Amst)*, **9**, 1283–1291.
4. Hopfner,K.P., Karcher,A., Craig,L., Woo,T.T., Carney,J.P. and Tainer,J.A. (2001) Structural biochemistry and interaction architecture of the DNA double-strand break repair Mre11 nuclease and Rad50-ATPase. *Cell*, **105**, 473–485.

5. Hopfner,K.P., Craig,L., Moncalian,G., Zinkel,R.A., Usui,T., Owen,B.A., Karcher,A., Henderson,B., Bodmer,J.L., McMurray,C.T. *et al.* (2002) The Rad50 zinc-hook is a structure joining Mre11 complexes in DNA recombination and repair. *Nature*, **418**, 562–566.
6. Connelly,J.C. and Leach,D.R. (1996) The *sbcC* and *sbcD* genes of *Escherichia coli* encode a nuclease involved in palindrome inviability and genetic recombination. *Genes Cells*, **1**, 285–291.
7. Connelly,J.C., de Leau,E.S., Okely,E.A. and Leach,D.R. (1997) Overexpression, purification, and characterization of the SbcCD protein from *Escherichia coli*. *J. Biol. Chem.*, **272**, 19819–19826.
8. Connelly,J.C., Kirkham,L.A. and Leach,D.R. (1998) The SbcCD nuclease of *Escherichia coli* is a structural maintenance of chromosomes (SMC) family protein that cleaves hairpin DNA. *Proc. Natl. Acad. Sci. U.S.A.*, **95**, 7969–7974.
9. Kamble,V.A. and Misra,H.S. (2010) The SbcCD complex of *Deinococcus radiodurans* contributes to radioresistance and DNA strand break repair *in vivo* and exhibits Mre11-Rad50 type activity in vitro. *DNA Repair (Amst)*, **9**, 488–494.
10. Hopfner,K.P., Karcher,A., Shin,D., Fairley,C., Tainer,J.A. and Carney,J.P. (2000) Mre11 and Rad50 from *Pyrococcus furiosus*: Cloning and biochemical characterization reveal an evolutionarily conserved multiprotein machine. *J. Bacteriol.*, **182**, 6036–6041.
11. Paull,T.T. and Gellert,M. (1998) The 3′ to 5′ exonuclease activity of Mre 11 facilitates repair of DNA double-strand breaks. *Mol. Cell*, **1**, 969–979.
12. Paull,T.T. and Gellert,M. (1999) Nbs1 potentiates ATP-driven DNA unwinding and endonuclease cleavage by the Mre11/Rad50 complex. *Genes Dev.*, **13**, 1276–1288.
13. Cannavo,E. and Cejka,P. (2014) Sae2 promotes dsDNA endonuclease activity within Mre11-Rad50-Xrs2 to resect DNA breaks. *Nature*, **514**, 122–125.
14. Leach,D.R., Okely,E.A. and Pinder,D.J. (1997) Repair by recombination of DNA containing a palindromic sequence. *Mol. Microbiol.*, **26**, 597–606.
15. Eykelenboom,J.K., Blackwood,J.K., Okely,E. and Leach,D.R. (2008) SbcCD causes a double-strand break at a DNA palindrome in the *Escherichia coli* chromosome. *Mol. Cell*, **29**, 644–651.
16. Leach,D.R. (1994) Long DNA palindromes, cruciform structures, genetic instability and secondary structure repair. *Bioessays*, **16**, 893–900.
17. Chalker,A.F., Leach,D.R. and Lloyd,R.G. (1988) *Escherichia coli sbcC* mutants permit stable propagation of DNA replicons containing a long palindrome. *Gene*, **71**, 201–205.
18. Bikard,D., Loot,C., Baharoglu,Z. and Mazel,D. (2010) Folded DNA in action: Hairpin formation and biological functions in prokaryotes. *Microbiol. Mol. Biol. Rev.*, **74**, 570–588.
19. Farah,J.A., Cromie,G., Steiner,W.W. and Smith,G.R. (2005) A novel recombination pathway initiated by the Mre11/Rad50/Nbs1 complex eliminates palindromes during meiosis in *Schizosaccharomyces pombe*. *Genetics*, **169**, 1261–1274.
20. Darmon,E., Eykelenboom,J.K., Lincker,F., Jones,L.H., White,M., Okely,E., Blackwood,J.K. and Leach,D.R. (2010) *E. coli* SbcCD and RecA control chromosomal rearrangement induced by an interrupted palindrome. *Mol. Cell*, **39**, 59–70.
21. Inagaki,H., Ohye,T., Kogo,H., Tsutsumi,M., Kato,T., Tong,M., Emanuel,B.S. and Kurahashi,H. (2013) Two sequential cleavage reactions on cruciform DNA structures cause palindrome-mediated chromosomal translocations. *Nat. Commun.*, **4**, 1592.
22. Azeroglu,B., Lincker,F., White,M.A., Jain,D. and Leach,D.R. (2014) A perfect palindrome in the *Escherichia coli* chromosome forms DNA hairpins on both leading- and lagging-strands. *Nucleic Acids Res.*, **42**, 13206–13213.
23. Higuchi,K., Katayama,T., Iwai,S., Hidaka,M., Horiuchi,T. and Maki,H. (2003) Fate of DNA replication fork encountering a single DNA lesion during *oriC* plasmid DNA replication *in vitro*. *Genes Cells*, **8**, 437–449.
24. Pinder,D.J., Blake,C.E., Lindsey,J.C. and Leach,D.R. (1998) Replication strand preference for deletions associated with DNA palindromes. *Mol. Microbiol.*, **28**, 719–727.
25. Kurahashi,H., Inagaki,H., Yamada,K., Ohye,T., Taniguchi,M., Emanuel,B.S. and Toda,T. (2004) Cruciform DNA structure underlies the etiology for palindrome-mediated human chromosomal translocations. *J. Biol. Chem.*, **279**, 35377–35383.
26. Ausubel,F.M., Brent,R., Kingston,R.E., Moore,D.D. and Seidman,J.G. (1994) *Current Protocols in Molecular Biology*. John Wiley & Sons, NY.
27. Mizuuchi,K., Mizuuchi,M. and Gellert,M. (1982) Cruciform structures in palindromic DNA are favored by DNA supercoiling. *J. Mol. Biol.*, **156**, 229–243.
28. Connelly,J.C., de Leau,E.S. and Leach,D.R. (1999) DNA cleavage and degradation by the SbcCD protein complex from *Escherichia coli*. *Nucleic Acids Res.*, **27**, 1039–1046.
29. Connelly,J.C., de Leau,E.S. and Leach,D.R. (2003) Nucleolytic processing of a protein-bound DNA end by the *E. coli* SbcCD (MR) complex. *DNA Repair (Amst)*, **2**, 795–807.
30. Moreau,S., Ferguson,J.R. and Symington,L.S. (1999) The nuclease activity of Mre11 is required for meiosis but not for mating type switching, end joining, or telomere maintenance. *Mol. Cell. Biol.*, **19**, 556–566.
31. Buis,J., Wu,Y., Deng,Y., Leddon,J., Westfield,G., Eckersdorff,M., Sekiguchi,J.M., Chang,S. and Ferguson,D.O. (2008) Mre11 nuclease activity has essential roles in DNA repair and genomic stability distinct from ATM activation. *Cell*, **135**, 85–96.
32. Arthur,L.M., Gustausson,K., Hopfner,K.P., Carson,C.T., Stracker,T.H., Karcher,A., Felton,D., Weitzman,M.D., Tainer,J. and Carney,J.P. (2004) Structural and functional analysis of Mre11–3. *Nucleic Acids Res.*, **32**, 1886–1893.
33. Williams,R.S., Moncalian,G., Williams,J.S., Yamada,Y., Limbo,O., Shin,D.S., Groocock,L.M., Cahill,D., Hitomi,C., Guenther,G. *et al.* (2008) Mre11 dimers coordinate DNA end bridging and nuclease processing in double-strand-break repair. *Cell*, **135**, 97–109.
34. Bhaskara,V., Dupre,A., Lengsfeld,B., Hopkins,B.B., Chan,A., Lee,J.H., Zhang,X., Gautier,J., Zakian,V. and Paull,T.T. (2007) Rad50 adenylate kinase activity regulates DNA tethering by Mre11/Rad50 complexes. *Mol. Cell*, **25**, 647–661.